Renewable and Sustainable Energy Reviews 56 (2016) 246–260

Contents lists available at ScienceDirect

Renewable and Sustainable Energy Reviews

journal homepage: www.elsevier.com/locate/rser

Evaluation of empirical models for predicting monthly mean horizontal diffuse solar radiation

Milan Despotovic [a,*], Vladimir Nedic [a], Danijela Despotovic [b], Slobodan Cvetanovic [c]

[a] Faculty of Engineering, University of Kragujevac, Kragujevac, Serbia
[b] Faculty of Economics, University of Kragujevac, Kragujevac, Serbia
[c] Faculty of Economics, University of Nis, Nis, Serbia

ARTICLE INFO

Article history:
Received 26 August 2015
Received in revised form
11 November 2015
Accepted 22 November 2015

Keywords:
Solar energy
Solar radiation models
Empirical models
Diffuse radiation
Model comparison

ABSTRACT

In many solar applications knowing diffuse solar radiation on horizontal surface represents an important requirement. The measurement of diffuse radiation is quite expensive, and because of that solar radiation measurements are not easily available in many locations around the world. Therefore many empirical correlations have been developed by various researchers to predict diffuse radiation from available meteorological data. The main objective of this study is to assess and compare different diffuse solar models available in the literature. These empirical models have been derived for specific location using long term measurements for that location. There is no general formula to calculate the diffuse solar radiation at any location in the world. While there are several studies in which authors compare different diffuse models for specific location, there is no comprehensive study in which these models are compared on a global scale. In this study we used statistical analysis to evaluate performance of analyzed models using long term measurements at 267 different sites around the world. Ten statistical quantitative indicators are used to evaluate different diffuse solar radiation models. The results are also visually presented by means of Taylor diagrams, which give a clear picture of how close a particular model is to measured data and how it is relatively compared to other models.

Contents

1. Introduction

Solar energy is being widely considered as important energy source for the future due to the environmental issues associated with the use of fossil fuels as well as their limited reserves. For the prediction, study, and design of solar energy systems, availability of a complete and accurate data on solar radiation and its components at a given location is essential [1]. Ideally, such information should be obtained from a dense network of stations where global, direct and diffuse radiations are routinely measured [2]. However, for many countries, particularly for developing ones, solar radiation measurements are not easily available [3]. On the other hand, while information exists on global solar radiation, the

* Corresponding author. Tel.: +381 69 844 9679.
E-mail address: mdespotovic@kg.ac.rs (M. Despotovic).

http://dx.doi.org/10.1016/j.rser.2015.11.058
1364-0321/

Nomenclature

Acronyms

erMAX	Maximum absolute relative error
MAE	Mean absolute error (kWh/m^2)
MARE	Mean absolute relative error
MBE	Mean bias error (kWh/m^2)
RMSE	Root mean squared error (kWh/m^2)
RMSRE	Root mean squared relative error
RRMSE	Relative root mean square error (%)

Greek Symbols

δ	Solar declination (°)
ω_{ss}	Sunset hour angle (°)
ϕ	Latitude (°)

Roman Symbols

n	Total number of observations
$\overline{H}_d^{i,c}$	ith calculated value (kWh/m^2)
$\overline{H}_d^{i,m}$	ith measured value (kWh/m^2)
$\overline{H}_d^{m,avg}$	Average of the measured value (kWh/m^2)
H	Monthly average daily global solar radiation (Wh/m^2)
H_0	Monthly average daily extraterrestrial radiation (Wh/m^2)
H_d	Monthly average daily diffuse solar radiation (Wh/m^2)
I_c	Solar constant (=1367 W/m^2)
$K_T(=H/H_0)$	Monthly average daily clearness index
N_d	The number of the day corresponding to a given date
R^2	R squared
S	Monthly average daily sunshine duration (h)
S_0	Monthly average maximum possible daily sunshine duration (h)
t-stat	t-Statistic
U_{95}	Uncertainty at 95% (kWh/m^2)

measurement of diffuse data is relatively more tedious and more expensive, and it is carried out at relatively few stations [4,5]. Thus, many empirical correlations have been developed by various researchers to predict diffuse radiation for locations where no measured data are available. There are two categories of solar radiation models, available in the literature, based on other more readily measured quantities: parametric models in which detailed information of atmospheric conditions is required and decomposition models which usually use information only on global radiation for the estimation of direct and diffuse component [6].

From pioneer work of Liu and Jordan [7] who presented empirical relationships between daily diffuse to daily total radiation and monthly average daily diffuse to monthly average daily total solar radiation, a lot of papers have been published in which authors presented further decomposition models that are obtained by fitting datasets from different locations and time periods. Tapakis et al. [8] recently reviewed this topic. Most decomposition models relate the diffuse fraction (ratio of diffuse solar radiation to global solar radiation) as a function of the clearness index (ratio of global solar radiation to extraterrestrial radiation), relative sunshine duration or a combination of them with varying degree order polynomials [9]. However, as cited in [10] "although these models are typically derived following sound approaches, their performance appears to lessen once they are applied to regions other than those, which provided the initial data for model development".

There are several studies in which authors compare different diffuse models for specific location, for example: Amritsar, India [11], Azores region (Graciosa Island) [12], Tabass, Iran [13], Pamplona, Spain [14], 22 locations in South Korea [15]. However, there is no comprehensive study in which these models are compared on a global scale, which could assist in the selection of most appropriate and accurate model based on the available measured meteorological data. In this study we used statistical analysis to evaluate performance of analyzed models using long term measurements at 267 different sites around the world. These sites are classified in five groups according to similar climatic conditions. Ten statistical quantitative indicators are used to evaluate different diffuse solar radiation models. These indicators are: mean absolute error (MAE), root mean squared error (RMSE), mean absolute relative error (MARE), uncertainty at 95% (U_{95}), root mean squared relative error (RMSRE), relative root mean square error (RRMSE), mean bias error (MBE), coefficient of determination (R^2), maximum absolute relative error (erMAX) and t-Statistic (t-stat). The results are also visually presented by means of Taylor diagrams, which give a clear picture of how close a particular model is to measured data and how it is relatively compared to other models.

2. Theoretical background

The monthly average daily extraterrestrial solar radiation on a horizontal surface is calculated from the following equation [16]:

$$H_0 = \frac{24 I_c}{\pi}\left[1+0.034\ \cos\left(360 N_d/365\right)\right] \times\left(\cos\phi\ \cos\delta\ \sin\omega_{ss}+\frac{2\pi\omega_{ss}}{360}\sin\phi\ \sin\delta\right) \quad (1)$$

where I_c is the solar constant (=1367 W/m^2), ϕ is the latitude of the site, N_d is day of the year starting from January 1st (Table 1), and δ and ω_{ss} are the monthly mean daily solar declination and sunrise hour angle given, respectively, as [17]:

$$\delta = 23.45\ \sin\left(360\frac{284+N_d}{365}\right) \quad (2)$$

$$\omega_{ss} = \cos^{-1}(-\tan\delta\ \tan\phi) \quad (3)$$

Table 1
Recommended average day for each month according to Klein [18].

Month	Date	N_d	Month	Date	N_d
January	17	17	July	17	198
February	16	47	August	16	228
March	16	75	September	15	258
April	15	105	October	15	288
May	15	135	November	14	318
June	11	162	December	10	344

Table 2
Review of different diffuse solar radiation models.

No.	Model	Year	Period	Location	Longitude	Latitude	Altitude	Climate Zone	Main Climate Zone
1	I-1	1961	Long term	10 Widely spread sites		−40 to 40			A, B, C
2	I-2	1985	1969–1977	Cairo, Egypt	31.3	30.1	112	BWh	B
3	I-3	1985	1969–1977	Cairo, Egypt	31.3	30.1	112	BWh	B
4	I-4	1977	1952–1956	Blue Hill, Massachusetts	−71.1	42.2	194	Dfa	D
5	I-5	1979	1964–1975	Combined Toronto–Montreal data, (Canada)	−79.5, −73.6	43.8, 45.5	76, 233	Dfb, Dfc	D
6	I-6	1979	1962–1975	Combined Toronto–Montreal–Goose Bay data, (Canada)	−79.5, −73.6, −60.5	43.8, 45.5, 53.3	76, 233, 12	Dfb, Dfc	D
7	I-7	1994	1988–1992	Gebze, Turkey	29.5	40.8	182	BWh	B
8	I-8	1994	1988–1992	Gebze, Turkey	29.5	40.8	182	BWh	B
9	I-9	1994	1988–1992	Gebze, Turkey	29.5	40.8	182	BWh	B
10	I-10	1994	1988–1992	Gebze, Turkey	29.5	40.8	182	BWh	B
11	I-11	2013	2004–2007	41 Sites, located in 11 EU countries	−10.3 to 37.6	37.1 to 59.4		BSk, Cfb, Csa, Csb, Dfb, ET	B, C, D, E
12	I-12	1999	1982–1989	AL-Arish, AL-Tahrir and Marsa Matroh (North Egypt); Cairo (Middle Egypt); AL-Kharga and Aswan (South Egypt)	27.2 to 33.9	24 to 31.3	23-194	BWh	B
13	I-13	1999	1982–1989	AL-Arish, AL-Tahrir and Marsa Matroh (North Egypt); Cairo (Middle Egypt); AL-Kharga and Aswan (South Egypt)	27.2 to 33.9	24 to 31.3	23-194	BWh	B
14	I-14	1991	1982–1985	Five regions in Turkey (Ankara, Antalya, Diyarbakir, Istanbul and Izmir)	27.2 to 40.2	36.5 to 41	30-840	Csa, Csb	C
15	I-15	2006	1990–1996	12 Provinces in the CAR, Turkey	30.3 to 47	37.5 to 40.4	751-1298	BSk, Cfa, Csa, Csb	B, C
16	I-16	2006	1990–1996	12 Provinces in the CAR, Turkey	30.3 to 47	37.5 to 40.4	751-1298	BSk, Cfa, Csa, Csb	B, C
17	I-17	2006	1990–1996	12 Provinces in the CAR, Turkey	30.3 to 47	37.5 to 40.4	751-1298	BSk, Cfa, Csa, Csb	B, C
18	I-18	2009	1990–2006	3 Big cities in Turkey (Ankara, Istanbul, Izmir)	32.9, 29.1, 27.2	40, 41, 38.4	894, 39, 15	Csa, Csb	C
19	I-19	2009	1990–2006	3 Cities in Turkey (Ankara, Istanbul, Izmir)	32.9, 29.1, 27.2	40, 41, 38.4	894, 39, 15	Csa, Csb	C
20	I-20	2005	1997–2001	5 Provinces (Amasya, Corum, Ordu, Samsun and Tokat) in the CSB Region of Turkey	34.6 to 37.5	40.2 to 41.2	4-798	Cfb, Csb	C
21	I-21	2005	1997–2001	5 Provinces (Amasya, Corum, Ordu, Samsun and Tokat) in the CSB Region of Turkey	34.6 to 37.5	40.2 to 41.2	4-798	Cfb, Csb	C
22	II-1	1996	1988–1992	Gebze, Turkey	29.4	40.8	182	Bwh	B
23	II-2	1981	1968–1976	Palermo, Italy	13.4	38.1	55	Csa	C
24	II-3	1981	1958–1973	Macerata, Italy	13.5	43.4	338	Cfb	C
25	II-4	1981	1958–1969	Genova, Italy	8.9	44.4	55	Csb	C
26	II-5	1985	1969–1977	Cairo, Egypt	31.3	30.1	112	BWh	B
27	II-6	2009	2001–2005	4 Locations in India (Jodhpur, Calcutta, Bombay, Pune)	72.9 to 88.4	18.5 to 26.3	112	Aw, BSh	A, B
28	II-7	1999	1982–1989	AL-Arish, AL-Tahrir and Marsa Matroh (North Egypt); Cairo (Middle Egypt); AL-Kharga and Aswan (South Egypt)	27.2 to 33.9	24 to 31.3	23-194	BWh	B
29	II-8	1983	1956–1978	Salisbury and Bulawayo in Zimbabwe	31, 28.6	−17.8, −20.2	1471, 1343	BSh, Cwb	B, C
30	II-9	1988	1957–1978	Delhi, Madras, and Poona, India	73.9 to 80.3	13 to 28.6	6-560	Aw, Cwa	A, C
31	II-10	2004	1994–1998	16 Stations all over China	76.1 to 127	17.8 to 48.4	6-560	Aw, BSk, BWk, Cfa, Cwa, Cwb, Dwa, Dwb, Dwc	A, B, C, D
32	II-11	1991	1982–1985	Five regions in Turkey (Ankara, Antalya, Diyarbakir, Istanbul and Izmir)	27.2 to 40.2	36.5 to 41	30-840	Csa, Csb	C
33	II-12	1998	1989–1990	Tripoli, Libya	13.2	32.9	80	BSh	B
34	II-13	2006	1990–1996	12 Provinces in the CAR, Turkey	30.3 to 47	37.5 to 40.4	751-1298	BSk, Cfa, Csa, Csb	B, C
35	II-14	2006	1990–1996	12 Provinces in the CAR, Turkey	30.3 to 47	37.5 to 40.4	751-1298	BSk, Cfa, Csa, Csb	B, C
36	II-15	2006	1990–1996	12 Provinces in the CAR, Turkey	30.3 to 47	37.5 to 40.4	751-1298	BSk, Cfa, Csa, Csb	B, C
37	II-16	2009	1990–2006	3 Big cities in Turkey (Ankara, Istanbul, Izmir)	32.9, 29.1, 27.2	40, 41, 38.4	894, 39, 15	Csa, Csb	C
38	II-17	2009	1990–2006	3 Big cities in Turkey (Ankara, Istanbul, Izmir)	32.9, 29.1, 27.2	40, 41, 38.4	894, 39, 15	Csa, Csb	C
39	II-18	2014	1985–2005	Isfahan, Iran	51.7	32.6	1550	BSk	B
40	II-19	2014	1990–2010	Six Algerian stations: Algiers, Constantine, Ghardaia, Bechar, Adrar, and Tamanrasset	−2.15 to 6.6	22.8 to 36.4	25-1377	BWh, Csa	B, C
41	III-1	2009	1995–2004	Eight typical cities in China (Haerbin, Lanzhou, Beijing, Wuhan, Kunming, Guangzhou, Wulumuqi, Lasa)	87.7 to 126.8	23.2 to 45.8	23-3648	BSk, Cfa, Cwa, Cwb, Dwa, Dwc	B, C, D
42	III-2	2009	1995–2004	Eight typical cities in China (Haerbin, Lanzhou, Beijing, Wuhan, Kunming, Guangzhou, Wulumuqi, Lasa)	87.7 to 126.8	23.2 to 45.8	23–3648	BSk, Cfa, Cwa, Cwb, Dwa, Dwc	B, C, D
43	III-3	1999	1982–1989	AL-Arish, AL-Tahrir and Marsa Matroh (North Egypt); Cairo (Middle Egypt); AL-Kharga and Aswan (South Egypt)	27.2 to 33.9	24 to 31.3	23-194	BWh	B

44	III-4	1995	Several years	40 Widely spread locations in Asia, Africa, Europe, and North America in the latitude range 36°S to 60°N	−36 to 60	5-1571				A, B, C
45	III-5	2007	1999–2001	Aswan, Egypt	24	194	BWh			B
46	III-6	2011	1994–2004	Four stations (Changdu, Geer, Lasa and Naqu) in Tibet	29.7 to 32.5	3306-4507	Dwc, ET			D, E
47	III-7	1988	1957–1978	Delhi, Madras, and Poona, India	13 to 28.6	6-560	Aw, Cwa			A, C
48	III-8	2015	1975–2007	Eight stations (Adana, Ankara, Diyarbakir, Erzurum, Istanbul, Izmir, Samsun and Trabzon) in Turkey	36.6 to 41.2	20-1869	Cfa, Cfb, Csa, Csb, Dfb			C, D
49	III-9	2014	1988–2000	Tabass, Iran	33.6	711	BWh			B
50	III-10	1994	1957–1967	Shambat, Sudan	15.7	380	BWh			B

The monthly mean daily maximum possible sunshine duration is [17]:

$$S_0 = \frac{2}{15}\cos^{-1}(-\tan\delta\,\tan\phi) \tag{4}$$

3. Analyzed empirical models

The empirical models that are used in this study can be classified in three groups as follows:

I. *Group*: In this group, the monthly mean diffuse fraction is the function of the monthly mean clearness index ($K_T = H/H_0$):

Models $H_d/H = f(H/H_0)$

Model I-1: Page [19]

$$K = 1.0 - 1.13(K_T) \tag{5}$$

Model I-2: Ibrahim [20]

$$K = 0.86 - 0.86(K_T) \tag{6}$$

Model I-3: Ibrahim [20]

$$K = 0.636 - 0.279(K_T) - 0.194(K_T)^2 - 0.383(K_T)^3 \tag{7}$$

Model I-4: Klein [18] using data from Liu and Jordan [7]

$$K = 1.390 - 4.027(K_T) + 5.531(K_T)^2 - 3.108(K_T)^3 \tag{8}$$

Model I-5: Iqbal [21]

$$K = 0.958 - 0.982(K_T) \tag{9}$$

Model I-6: Iqbal [21]

$$K = 0.914 - 0.847(K_T) \tag{10}$$

Model I-7: Tiris et al. (as cited in [22])

$$K = 0.3917 + 0.0065\exp(1/(K_T)) \tag{11}$$

Model I-8: Tiris et al. (as cited in [22])

$$K = 0.6875 - 0.4981(K_T) \tag{12}$$

Model I-9: Tiris et al. (as cited in [22])

$$K = 0.2599 + 0.088(1/(K_T)) \tag{13}$$

Model I-10: Tiris et al. (as cited in [22])

$$K = 0.583 + 0.9985(K_T) - 5.24(K_T)^2 + 5.322(K_T)^3 \tag{14}$$

Model I-11: Bortolini et al. [23]

$$K = 0.9888 + 0.3950(K_T) - 3.7003(K_T)^2 + 2.2905(K_T)^3 \tag{15}$$

Model I-12: Trabea [24]

$$K = 0.924 - 0.894(K_T) \tag{16}$$

Model I-13: Trabea [24]

$$K = 0.534 + 0.384(K_T) - 1.036(K_T)^2 \tag{17}$$

Model I-14: Taşdemiroğlu and Sever [25]

$$K = 0.791 - 0.775(K_T) \tag{18}$$

Model I-15: Aras et al. [26]

$$K = 1.0212 - 1.1672(K_T) \tag{19}$$

Model I-16: Aras et al. [26]

$$K = 1.1244 - 1.5582(K_T) + 0.3635(K_T)^2 \tag{20}$$

Model I-17: Aras et al. [26]

$$K = 1.7111 - 4.9062(K_T) + 6.6711(K_T)^2 - 3.9235(K_T)^3 \tag{21}$$

Model I-18: Ulgen and Hepbasli [27]

$$K = 0.6772 - 0.4841(K_T) \tag{22}$$

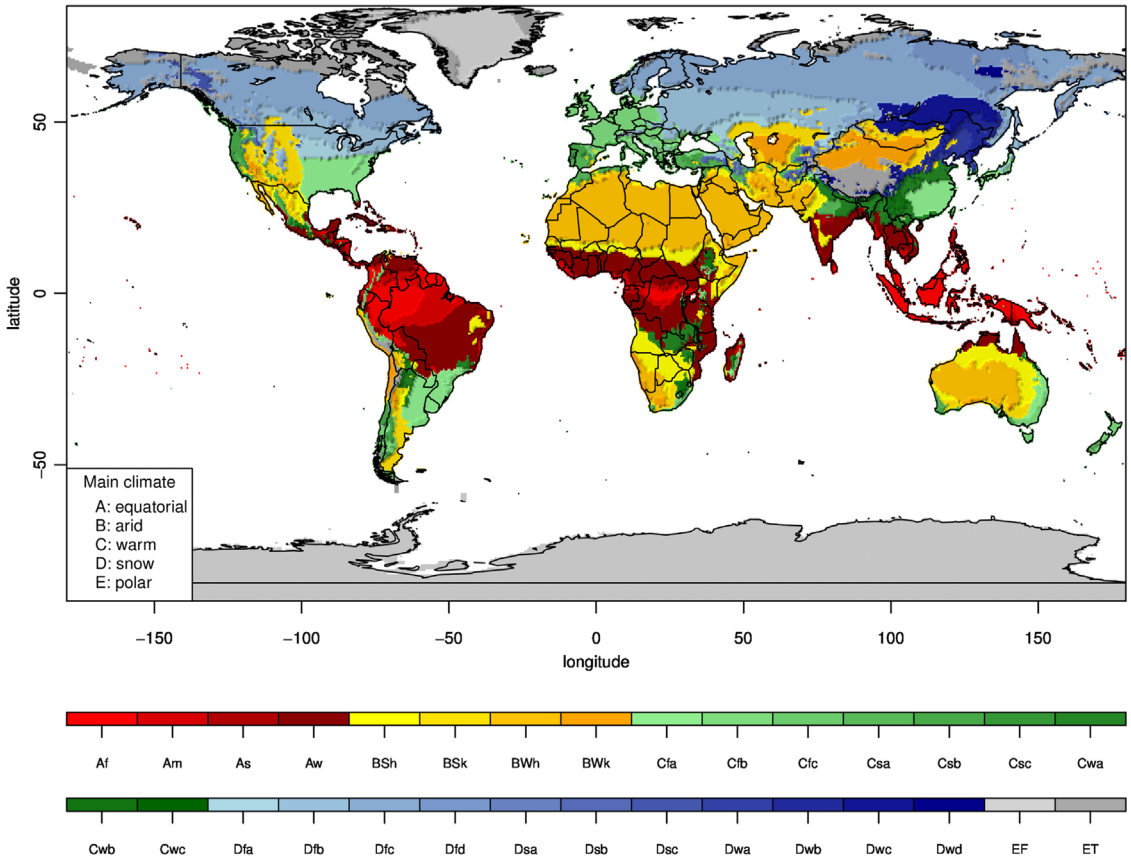

Fig. 1. World map of Köppen–Geiger climate classification.

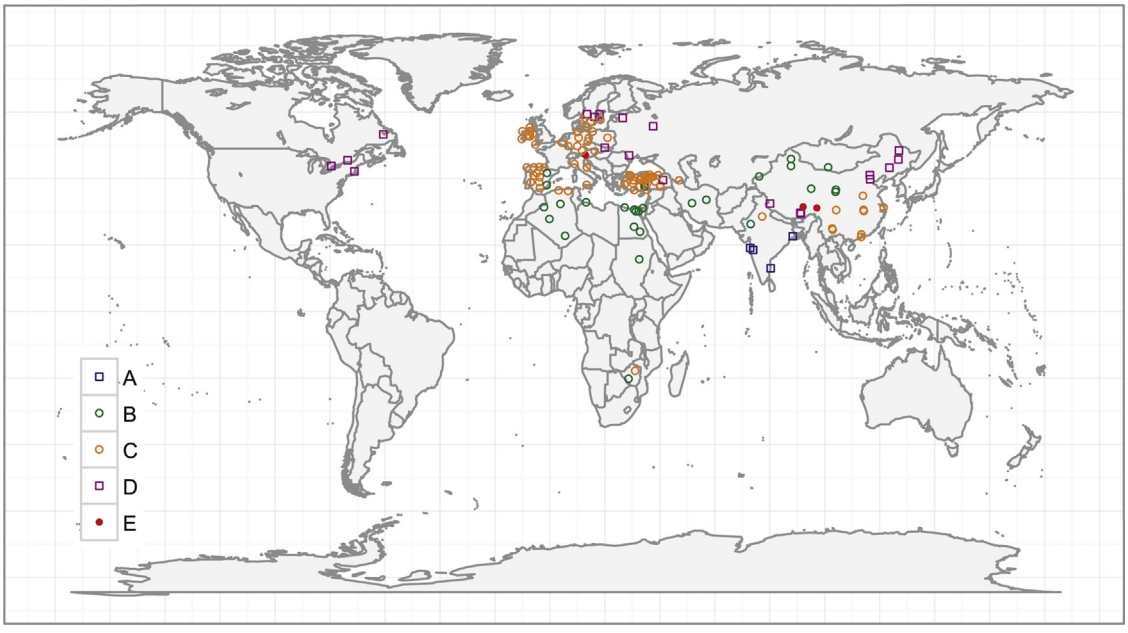

Fig. 2. Locations for which models were developed (legend denotes climate zones).

Model I-19: Ulgen and Hepbasli [27]

$$K = 0.981 - 1.9028(K_T) + 1.9319(K_T)^2 - 0.6809(K_T)^3 \quad (23)$$

Model I-20: Tarhan and Sari [28]

$$K = 1.0207 - 1.6582(K_T) + 1.1018(K_T)^2 - 0.4019(K_T)^3 \quad (24)$$

Model I-21: Tarhan and Sari [28]

$$K = 0.9885 - 1.4276(K_T) + 0.5679(K_T)^2 \quad (25)$$

II. *Group*: In this group, the monthly mean diffuse fraction is the function of the monthly mean relative sunshine duration (S/S_0):

Models $H_d/H = f(S/S_0)$

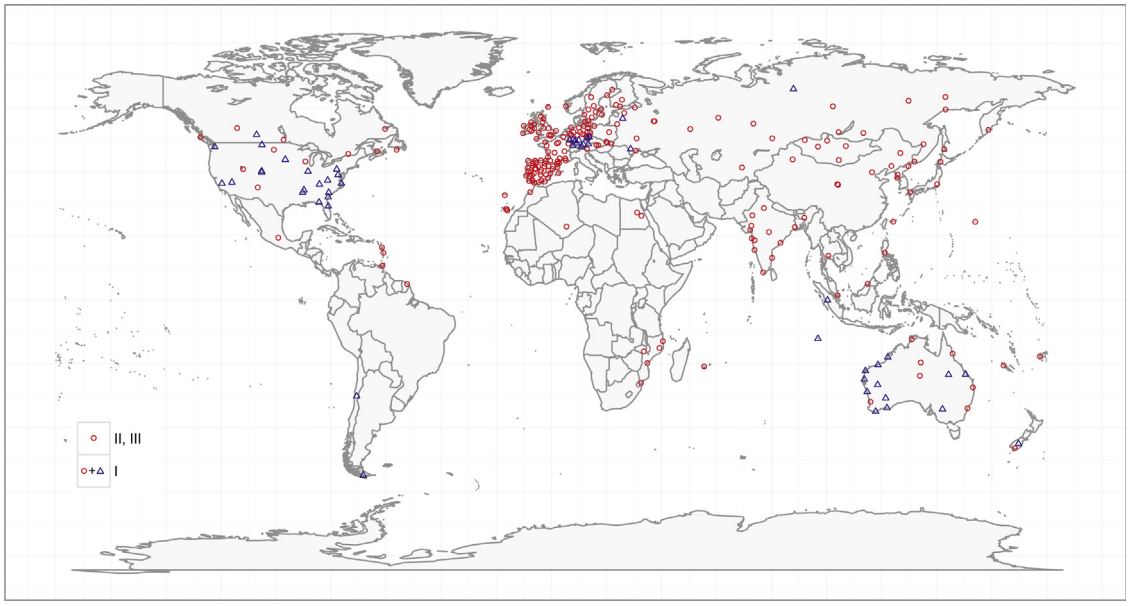

Fig. 3. Locations of sites used for the study (triangles denote missing sunshine duration).

Model II-1: Tiris et al. [22]

$$K = 0.4177 - 0.07702(S/S_0) - 1.9069(S/S_0)^2 - 1.19(S/S_0)^3 \quad (26)$$

Model II-2: Barbaro et al. [29]

$$K = 0.7434 - 0.8203(S/S_0) + 0.2454(S/S_0)^2 \quad (27)$$

Model II-3: Barbaro et al. [29]

$$K = 1.0297 - 2.1096(S/S_0) + 1.5193(S/S_0)^2 \quad (28)$$

Model II-4: Barbaro et al. [29]

$$K = 0.8159 - 1.3289(S/S_0) + 0.8668(S/S_0)^2 \quad (29)$$

Model II-5: Ibrahim [20]

$$K = 0.79 - 0.59(S/S_0) \quad (30)$$

Model II-6: Pandey and Katiyar [30]

$$K = 0.9781 + 4.763(S/S_0) - 11.32(S/S_0)^2 + 7.167(S/S_0)^3 \quad (31)$$

Model II-7: Trabea [24]

$$K = 0.896 - 0.688(S/S_0) \quad (32)$$

Model II-8: Lewis [31]

$$K = 0.754 - 0.654(S/S_0) \quad (33)$$

Model II-9: Gopinathan [32]

$$K = 0.931 - 0.814(S/S_0) \quad (34)$$

Model II-10: Rensheng et al. [33]

$$K = 0.95 - 0.60(S/S_0) - 0.20(S/S_0)^2 \quad (35)$$

Model II-11: Taşdemiroğlu and Sever [25]

$$K = 0.622 - 0.350(S/S_0) \quad (36)$$

Model II-12: Said et al. [34]

$$K = 1.625 - 3.421(S/S_0) + 2.185(S/S_0)^2 \quad (37)$$

Model II-13: Aras et al. [26]

$$K = 0.663 - 0.4883(S/S_0) \quad (38)$$

Model II-14: Aras et al. [26]

$$K = 0.6492 - 0.4323(S/S_0) - 0.0512(S/S_0)^2 \quad (39)$$

Model II-15: Aras et al. [26]

$$K = 0.5562 + 0.1536(S/S_0) - 1.2027(S/S_0)^2 + 0.7122(S/S_0)^3 \quad (40)$$

Model II-16: Ulgen and Hepbasli [27]

$$K = 0.5456 - 0.2242(S/S_0) \quad (41)$$

Model II-17: Ulgen and Hepbasli [27]

$$K = 0.6595 - 0.7841(S/S_0) + 0.7461(S/S_0)^2 - 0.2579(S/S_0)^3 \quad (42)$$

Model II-18: Sabzpooshani and Mohammad [35]

$$K = -0.59276 + 4.60382(S/S_0) - 6.85670(S/S_0)^2 + 3.06795(S/S_0)^3 \quad (43)$$

Model II-19: Boukelia et al. [36]

$$K = 0.337 - 0.068(S/S_0) + 0.025(S/S_0)^2 - 0.002(S/S_0)^3 \quad (44)$$

III. *Group*: In this group, the monthly mean diffuse fraction is the function of the monthly mean clearness index and the relative sunshine duration:

Models $H_d/H = f(H/H_0, S/S_0)$

Model III-1: Jiang [37]

$$K = 0.945 - 0.675(K_T) - 0.166(K_T)^2 - 0.173(S/S_0) - 0.079(S/S_0)^2 \quad (45)$$

Model III-2: Jiang [37]

$$K = 1 - 0.858(K_T) - 0.235(S/S_0) \quad (46)$$

Model III-3: Trabea [24]

$$K = 0.927 - 0.164(K_T) - 0.595(S/S_0) \quad (47)$$

Model III-4: Gopinathan and Soler [38]

$$K = 0.87813 - 0.33280(K_T) - 0.53039(S/S_0) \quad (48)$$

Model III-5: Elminir et al. [39]

$$K = 0.7980 - 0.7475(K_T) - 0.0702(S/S_0) \quad (49)$$

Model III-6: Li et al. [40]

$$K = 0.7463 + 1.2922(K_T) - 3.7966(K_T)^2 - 0.7285(S/S_0) + 1.0592(S/S_0)^2 \quad (50)$$

Model III-7: Gopinathan [32]

$$K = 1.194 - 0.838(K_T) - 0.446(S/S_0) \quad (51)$$

Model III-8: Bakirci [4]

$$K = 0.8130 - 0.2041(K_T) - 0.8108(K_T)^2 + 0.5217(K_T)^3 - 0.0491(S/S_0) - 0.5646(S/S_0)^2 - 0.3961(S/S_0)^3 \quad (52)$$

Model III-9: Khorasanizadeh et al. [13]

$$K = 0.9593 - 0.8713(K_T) + 0.29191(K_T)^2 - 0.0979(K_T)^3 - 0.28419(S/S_0) + 0.02653(S/S_0)^2 - 0.02083(S/S_0)^3 \quad (53)$$

Model III-10: Omer [41]

$$K = 1.0 - 1.06(K_T) - 0.05(S/S_0) \quad (54)$$

Review of empirical models that are used in this study is given in Table 2. This table summarizes original locations/regions for which each empirical model was developed. Altitude is given in meters (m), and longitude and latitude in degrees (°), while positive values refer to east and north respectively and negative values to west and south respectively. In addition, Table 2 shows climate zones related to locations/regions for which each empirical model was developed. These zones are determined using Köppen–Geiger climate classification, which is the most frequently used climate classification system [42]. The Köppen–Geiger climate classification divides climates into five main zones: equatorial (A), arid (B), warm (C), snow (D) and polar (E). Each of these main climate zones have several subtypes depending on precipitation and air temperature. The world map of Köppen–Geiger climate classification is given in Fig. 1 and locations for which analyzed models were developed in Fig. 2.

4. Test data

The empirical models described in the previous section are evaluated using meteorological data from the World Radiation Data Centre (WRDC) [43]. WRDC is sponsored by the World Meteorological Organization and serves as a central depository for solar radiation data collected from different places in the world. The WRDC archive contains data on solar radiation, radiation balance and sunshine duration that covers the period from 1955 to

Table 3
Statistical indicators for empirical models for climate zone A.

#	MAE	RMSE	MARE	U_{95}	RMSRE	RRMSE	R^2	erMAX	MBE	*t*-stat
1	0.251	0.329	0.111	0.857	0.141	15.357	0.538	0.502	0.161	9.897
2	0.256	0.341	0.114	0.915	0.144	15.922	0.504	0.440	0.124	6.866
3	0.331	0.432	0.140	1.058	0.169	20.156	0.204	0.398	0.287	15.668
4	0.421	0.509	0.180	1.176	0.203	23.764	−0.106	0.404	0.399	22.272
5	0.246	0.307	0.120	0.849	0.154	14.330	0.598	0.572	−0.039	2.243
6	0.327	0.387	0.169	1.004	0.213	18.036	0.363	0.625	−0.192	10.067
7	0.433	0.525	0.217	1.441	0.277	24.482	−0.174	1.089	−0.107	3.678
8	0.326	0.409	0.157	1.134	0.198	19.067	0.288	0.703	−0.004	0.190
9	0.379	0.466	0.187	1.288	0.238	21.719	0.076	0.927	−0.050	1.889
10	0.501	0.627	0.259	1.700	0.354	29.242	−0.675	1.648	−0.187	5.527
11	0.346	0.432	0.176	1.030	0.232	20.147	0.205	0.916	−0.311	18.357
12	0.282	0.341	0.142	0.920	0.181	15.895	0.505	0.586	−0.111	6.075
13	0.302	0.368	0.149	1.009	0.184	17.148	0.424	0.526	−0.075	3.651
14	0.308	0.408	0.131	1.028	0.161	19.033	0.291	0.375	0.241	12.895
15	0.249	0.326	0.111	0.850	0.141	15.193	0.548	0.517	0.156	9.653
16	0.248	0.324	0.110	0.845	0.141	15.107	0.553	0.521	0.156	9.665
17	0.247	0.322	0.110	0.840	0.140	15.008	0.559	0.523	0.154	9.633
18	0.326	0.412	0.157	1.142	0.197	19.207	0.277	0.701	0.009	0.402
19	0.339	0.427	0.163	1.183	0.208	19.906	0.224	0.811	0.015	0.610
20	0.273	0.364	0.119	0.952	0.149	16.990	0.435	0.405	0.173	9.523
21	0.274	0.364	0.120	0.954	0.149	16.995	0.434	0.406	0.170	9.297
22	5.716	6.327	2.964	13.498	3.478	297.524	−169.630	10.722	5.716	36.413
23	0.381	0.453	0.169	1.028	0.192	21.290	0.126	0.385	0.368	24.029
24	0.439	0.516	0.196	1.230	0.224	24.266	−0.135	0.749	0.374	18.136
25	0.439	0.516	0.196	1.230	0.224	24.266	−0.135	0.749	0.374	18.136
26	0.238	0.298	0.120	0.802	0.156	14.032	0.620	0.524	−0.105	6.499
27	4.754	4.828	2.353	9.606	2.445	227.023	−98.347	5.432	−4.754	97.747
28	0.368	0.446	0.190	1.035	0.237	20.956	0.153	0.677	−0.345	21.089
29	0.322	0.388	0.148	0.919	0.174	18.240	0.359	0.407	0.285	18.762
30	0.251	0.314	0.126	0.834	0.161	14.748	0.581	0.471	−0.126	7.620
31	0.506	0.586	0.252	1.303	0.299	27.574	−0.466	0.755	−0.496	27.507
32	0.279	0.352	0.134	0.977	0.169	16.560	0.471	0.561	0.006	0.294
33	0.273	0.347	0.126	0.948	0.157	16.319	0.487	0.630	0.085	4.382
34	0.294	0.369	0.130	0.916	0.152	17.335	0.421	0.334	0.232	14.004
35	0.294	0.368	0.130	0.916	0.152	17.321	0.422	**0.334**	0.230	13.863
36	0.294	0.369	0.129	0.918	0.152	17.371	0.418	0.341	0.232	13.928
37	0.328	0.416	0.158	1.154	0.201	19.565	0.262	0.734	**0.004**	**0.148**
38	0.340	0.430	0.165	1.192	0.212	20.212	0.213	0.851	0.019	0.749
39	0.448	0.660	0.187	1.656	0.248	31.025	−0.855	0.877	0.397	13.043
40	0.583	0.728	0.249	1.717	0.289	34.254	−1.262	0.604	0.543	19.355
41	0.273	0.338	0.127	0.845	0.152	15.877	0.514	0.410	0.206	13.308
42	0.232	0.292	0.107	0.774	0.133	13.750	0.636	0.459	0.124	8.059
43	0.357	0.432	0.185	1.005	0.232	20.321	0.204	0.658	−0.333	20.950
44	0.265	0.325	0.123	0.815	0.148	15.285	0.550	0.367	0.197	13.159
45	0.363	0.451	0.156	1.064	0.180	21.192	0.134	0.381	0.335	19.189
46	0.814	0.918	0.399	2.057	0.457	43.173	−2.593	1.021	0.765	26.059
47	0.320	0.395	0.161	0.957	0.206	18.570	0.335	0.705	−0.272	16.386
48	1.158	1.372	0.600	3.060	0.757	64.502	−7.020	2.492	1.153	26.801
49	0.232	**0.292**	0.105	**0.772**	**0.127**	**13.742**	**0.636**	0.395	0.127	8.329
50	**0.230**	0.303	**0.104**	0.812	0.134	14.266	0.608	0.509	0.112	6.884

Table 4
Statistical indicators for empirical models for climate zone B.

#	MAE	RMSE	MARE	U_{95}	RMSRE	RRMSE	R^2	erMAX	MBE	*t*-stat
1	0.212	0.293	0.136	0.803	0.173	18.594	0.746	0.696	0.066	4.644
2	0.277	0.358	0.201	0.973	0.284	22.690	0.621	1.357	−0.099	5.823
3	0.231	0.320	0.147	0.870	0.186	20.312	0.697	0.741	0.093	6.095
4	0.269	0.363	0.170	0.960	0.211	23.028	0.610	0.805	0.156	9.582
5	0.322	0.395	0.235	1.014	0.320	25.018	0.540	1.411	−0.209	12.635
6	0.492	0.593	0.364	1.411	0.490	37.586	−0.039	2.113	−0.430	21.282
7	0.773	0.978	0.580	2.360	0.840	62.021	−1.829	4.480	−0.682	19.627
8	0.505	0.642	0.381	1.599	0.552	40.734	−0.220	2.815	−0.401	16.120
9	0.652	0.834	0.493	2.040	0.723	52.872	−1.056	3.890	−0.555	18.004
10	1.119	1.514	0.855	3.677	1.370	95.980	−5.775	9.006	−1.033	18.829
11	0.314	0.374	0.218	0.936	0.262	23.710	0.587	0.920	−0.228	15.474
12	0.407	0.496	0.302	1.218	0.411	31.433	0.273	1.800	−0.325	17.521
13	0.405	0.490	0.297	1.209	0.392	31.051	0.291	1.583	−0.315	16.990
14	0.269	0.353	0.191	0.980	0.267	22.410	0.631	1.310	**−0.019**	1.066
15	**0.209**	0.294	0.131	0.800	0.168	18.619	0.745	0.652	0.078	5.586
16	0.214	0.294	0.139	0.807	0.179	18.640	0.744	0.726	0.060	4.241
17	0.210	0.295	0.131	0.798	0.166	18.695	0.743	0.601	0.090	6.479
18	0.502	0.640	0.379	1.598	0.551	40.571	−0.211	2.827	−0.393	15.728
19	0.563	0.732	0.428	1.828	0.644	46.443	−0.586	3.582	−0.451	15.789
20	0.285	0.374	0.208	1.025	0.304	23.726	0.586	1.549	−0.083	4.602
21	0.295	0.390	0.218	1.065	0.326	24.758	0.549	1.768	−0.099	5.280
22	7.635	8.632	4.821	18.677	5.654	502.068	−194.575	16.187	7.635	29.309
23	0.307	0.390	0.173	0.949	0.200	22.665	0.601	0.438	0.264	14.265
24	0.419	0.523	0.263	1.448	0.351	30.446	0.281	1.555	0.057	1.692
25	0.419	0.523	0.263	1.448	0.351	30.446	0.281	1.555	0.057	1.692
26	0.265	0.331	0.169	0.870	0.225	19.272	0.712	0.758	−0.152	7.963
27	4.808	5.109	2.975	10.572	3.219	297.136	−67.501	8.239	−4.808	43.044
28	0.372	0.451	0.239	1.068	0.301	26.257	0.465	0.894	−0.333	16.877
29	0.297	0.379	0.167	0.908	0.202	22.055	0.623	0.471	0.271	15.769
30	0.229	**0.278**	0.143	**0.765**	0.173	**16.140**	**0.798**	0.489	−0.045	2.555
31	0.410	0.501	0.256	1.166	0.314	29.112	0.342	0.828	−0.384	18.530
32	0.329	0.422	0.213	1.117	0.292	24.536	0.533	0.993	−0.179	7.234
33	0.285	0.370	0.180	1.025	0.254	21.510	0.641	1.231	0.024	**1.005**
34	0.238	0.320	0.140	0.854	0.176	18.609	0.731	0.512	0.124	6.477
35	0.238	0.319	0.139	0.849	0.174	18.570	0.732	0.490	0.128	6.781
36	0.242	0.324	0.143	0.871	0.182	18.836	0.725	0.564	0.113	5.749
37	0.410	0.520	0.267	1.354	0.363	30.236	0.291	1.234	−0.253	8.609
38	0.448	0.571	0.294	1.486	0.405	33.199	0.145	1.444	−0.279	8.652
39	0.285	0.447	0.163	1.197	0.218	25.972	0.477	0.786	0.163	6.053
40	0.399	0.528	0.236	1.424	0.295	30.703	0.269	0.951	0.175	5.423
41	0.289	0.384	0.158	0.936	0.194	22.338	0.613	0.462	0.260	14.176
42	0.238	0.320	0.131	0.828	0.160	18.635	0.731	0.439	0.165	9.285
43	0.360	0.434	0.232	1.030	0.291	25.268	0.505	0.854	−0.319	16.686
44	0.266	0.344	0.149	0.843	0.180	19.989	0.690	**0.416**	0.227	13.552
45	0.292	0.395	0.159	0.988	0.190	22.988	0.590	0.507	0.242	11.990
46	1.070	1.323	0.629	3.015	0.753	76.934	−3.592	2.061	1.065	21.009
47	0.239	0.303	0.148	0.811	0.183	17.613	0.759	0.452	−0.112	6.183
48	1.713	1.997	1.076	4.404	1.298	116.167	−9.470	3.819	1.713	25.785
49	0.216	0.292	**0.123**	0.779	**0.151**	17.000	0.776	0.419	0.115	6.638
50	0.232	0.319	0.129	0.856	0.160	18.578	0.732	0.466	0.117	6.103

2013. However, although these data are freely accessible through WRDC website, their collecting is very troublesome since only data for one year per site is possible to download in one pass. Subdirectory structure of the web database and separate data sets for global radiation, diffuse radiation and sunshine duration additionally complicate the downloading of data. Therefore a Web crawler is written by means of which the needed data are fetched from the website. The period for which the data are available for different sites varies from one year to 65 years. The monthly average values of daily global radiation, daily diffuse radiation and daily sunshine duration for specific site are found as arithmetic means of readings during the period for which these data are available for that site. In order to avoid seasonal bias, all sites that do not have measurements for all 12 months were discarded from analysis. For I. group of empirical models 267 different sites are used for evaluation, while for II. and III. group of models 216 sites are used since some sites are missing data for sunshine duration. Locations of sites that are used for the study are shown in Fig. 3. In order to avoid biased analysis due to uneven distribution of sites, these sites are classified in five main climate zones according to Köppen–Geiger climate classification, and analysis was carried out for each zone separately.

5. Comparison methodology

In different studies in which solar models are compared, the model goodness is assessed by different statistical parameters. In order to enable some kind of compatibility in comparing results from previous work, we collected commonly used statistical parameters, so that, in this study, ten statistical quantitative indicators were used to evaluate different diffuse solar radiation models. Although fewer indicators are sufficient for such an evaluation, a comprehensive list of ten statistical indicators is given in order to provide readers a wider review. The quantitative indicators that are used in this paper are

1. *MAE*: mean absolute error. The MAE is the sum of absolute values of the errors divided by the number of observations. This

Table 5
Statistical indicators for empirical models for climate zone C.

#	MAE	RMSE	MARE	U_{95}	RMSRE	RRMSE	R^2	erMAX	MBE	*t*-stat
1	0.125	0.175	0.076	0.472	0.097	11.066	0.943	0.426	0.058	14.563
2	0.155	0.205	0.100	0.555	0.121	12.948	0.921	0.512	0.059	12.614
3	0.216	0.278	0.141	0.677	0.164	17.604	0.855	0.458	0.188	38.226
4	0.263	0.335	0.153	0.785	0.170	21.179	0.790	0.399	0.253	47.840
5	0.144	0.199	0.094	0.536	0.128	12.615	0.925	0.602	−0.068	15.197
6	0.208	0.296	0.134	0.755	0.186	18.708	0.836	0.904	−0.163	27.426
7	0.300	0.437	0.190	1.209	0.266	27.663	0.641	2.628	−0.045	4.333
8	0.229	0.309	0.155	0.856	0.197	19.521	0.821	1.435	0.006	**0.822**
9	0.266	0.377	0.174	1.045	0.234	23.857	0.733	2.218	−0.016	1.727
10	0.347	0.605	0.222	1.663	0.384	38.234	0.314	6.207	−0.106	7.398
11	0.334	0.382	0.229	0.850	0.253	24.156	0.726	0.781	−0.322	65.322
12	0.174	0.244	0.113	0.642	0.156	15.464	0.888	0.734	−0.111	21.073
13	0.198	0.260	0.138	0.712	0.172	16.435	0.873	0.738	−0.055	9.058
14	0.199	0.259	0.127	0.655	0.147	16.407	0.874	0.445	0.151	29.824
15	0.121	0.172	0.074	0.467	0.097	10.901	0.944	0.473	0.051	12.776
16	0.118	0.168	0.072	0.458	0.094	10.643	0.947	0.420	0.046	11.749
17	0.121	0.175	0.077	0.478	0.104	11.072	0.942	0.955	0.042	10.369
18	0.232	0.311	0.157	0.862	0.198	19.673	0.818	1.446	0.017	2.318
19	0.240	0.335	0.156	0.928	0.206	21.187	0.789	2.017	0.017	2.141
20	0.167	0.222	0.103	0.589	0.123	14.047	0.907	0.565	0.092	18.986
21	0.168	0.224	0.104	0.596	0.125	14.179	0.906	0.740	0.090	18.174
22	3.229	4.655	1.920	11.247	2.696	299.030	−39.823	22.322	3.229	36.069
23	0.195	0.250	0.122	0.603	0.139	16.070	0.882	0.613	0.175	36.578
24	0.269	0.358	0.158	0.922	0.201	23.009	0.758	2.514	0.188	23.111
25	0.269	0.358	0.158	0.922	0.201	23.009	0.758	2.514	0.188	23.111
26	0.189	0.265	0.122	0.662	0.164	17.012	0.868	0.987	−0.162	28.906
27	3.492	4.008	2.162	8.752	2.307	257.443	−29.258	11.672	−3.492	66.494
28	0.357	0.437	0.226	0.992	0.264	28.094	0.640	1.096	−0.356	52.383
29	0.132	0.182	0.083	0.469	0.101	11.671	0.938	0.446	0.093	22.413
30	0.245	0.305	0.163	0.707	0.189	19.615	0.824	0.774	−0.238	46.426
31	0.495	0.574	0.316	1.263	0.342	36.876	0.379	1.039	−0.494	63.412
32	0.210	0.288	0.143	0.798	0.187	18.512	0.844	1.524	−0.019	2.489
33	0.247	0.342	0.203	0.879	0.278	21.968	0.780	2.076	−0.182	23.482
34	0.164	0.216	0.111	0.565	0.133	13.878	0.912	0.725	0.101	19.845
35	0.164	0.215	0.111	0.563	0.134	13.815	0.913	0.664	0.101	19.873
36	0.166	0.218	0.115	0.570	0.141	13.973	0.911	0.985	0.101	19.527
37	0.265	0.356	0.183	0.987	0.232	22.887	0.761	1.908	0.013	1.408
38	0.269	0.373	0.179	1.034	0.236	23.969	0.738	2.215	0.023	2.281
39	0.425	0.559	0.339	1.365	0.445	35.912	0.411	1.358	0.374	33.758
40	0.494	0.596	0.338	1.411	0.373	38.298	0.330	1.571	0.439	40.810
41	0.113	0.172	0.069	0.462	0.094	11.055	0.944	0.679	0.062	14.384
42	**0.101**	0.147	0.065	0.407	0.087	9.440	0.959	0.440	**0.006**	1.491
43	0.341	0.417	0.218	0.944	0.253	26.769	0.673	0.964	−0.339	52.603
44	0.103	0.151	**0.064**	0.414	0.085	9.688	0.957	0.419	0.031	7.838
45	0.223	0.285	0.139	0.676	0.157	18.332	0.847	**0.364**	0.210	40.504
46	0.482	0.768	0.269	1.914	0.440	49.327	−0.111	5.303	0.476	29.578
47	0.335	0.385	0.231	0.857	0.250	24.754	0.720	0.649	−0.325	59.006
48	0.557	0.958	0.321	2.427	0.553	61.515	−0.728	5.560	0.549	26.183
49	0.104	**0.146**	0.066	**0.404**	**0.084**	**9.397**	**0.960**	0.387	0.018	4.523
50	0.110	0.156	0.069	0.428	0.089	10.006	0.954	0.375	0.027	6.697

quantity is often used in statistics as measure how close calculated values are to measured values. In [44] authors pointed out some advantages of MAE over the root mean squared error (RMSE) in dimensioned evaluations and inter-comparisons of average model performance error:

$$\mathrm{MAE} = \frac{1}{n}\sum_{i=1}^{n}\left|\overline{H}_d^{i,m} - \overline{H}_d^{i,c}\right| \tag{55}$$

2. *RMSE*: root mean squared error [44]. The RMSE is a frequently used measure to compare forecasting errors of different models. The lower RMSE value the better the predictive capability of a model in terms of its absolute deviation. However, presence of few large errors can result in greater value of RMSE:

$$\mathrm{RMSE} = \sqrt{\frac{1}{n}\sum_{i=1}^{n}\left(\overline{H}_d^{i,m} - \overline{H}_d^{i,c}\right)^2} \tag{56}$$

3. *MARE*: mean absolute relative error. The MARE when expressed in percentages is also known as mean absolute percentage error (MAPE) [45]. This indicator is expressed as average absolute value of relative differences between estimated and measured horizontal diffuse solar radiations:

$$\mathrm{MARE} = \frac{1}{n}\sum_{i=1}^{n}\left|\frac{\overline{H}_d^{i,m} - \overline{H}_d^{i,c}}{\overline{H}_d^{i,m}}\right| \tag{57}$$

4. U_{95}: Uncertainty at 95%. Following Gueymard [46] and Behar et al. [47], this indicator is used in order to show more information about the model deviation. Uncertainty with a 95% confidence level is given as

$$\mathrm{U_{95}} = 1.96(\mathrm{SD}^2 + \mathrm{RMSE}^2)^{1/2} \tag{58}$$

where 1.96 is the coverage factor corresponding 95% confidence level, and SD is the standard deviation of the difference between the calculated and measured data.

Table 6
Statistical indicators for empirical models for climate zone D.

#	MAE	RMSE	MARE	U_{95}	RMSRE	RRMSE	R^2	erMAX	MBE	t-stat
1	0.157	0.226	0.126	0.607	0.173	15.302	0.913	0.926	0.081	10.159
2	0.161	0.221	0.134	0.581	0.176	14.932	0.917	0.827	0.097	13.060
3	0.222	0.285	0.181	0.683	0.221	19.289	0.862	0.937	0.203	27.063
4	0.282	0.350	0.207	0.805	0.241	23.655	0.792	0.903	0.276	34.095
5	0.160	0.219	0.123	0.606	0.161	14.828	0.918	0.830	−0.022	2.634
6	0.191	0.258	0.136	0.690	0.172	17.460	0.887	0.750	−0.097	10.746
7	0.178	0.246	0.147	0.675	0.190	16.662	0.897	0.918	0.053	5.885
8	0.167	0.223	0.145	0.602	0.185	15.079	0.915	0.676	0.071	8.926
9	0.172	0.233	0.146	0.632	0.187	15.767	0.908	0.782	0.069	8.275
10	0.182	0.263	0.150	0.727	0.199	17.826	0.882	1.302	0.039	3.973
11	0.338	0.427	0.222	1.052	0.256	28.901	0.689	0.908	−0.277	22.711
12	0.171	0.232	0.127	0.634	0.164	15.676	0.909	0.784	−0.053	6.310
13	0.168	0.224	0.139	0.620	0.176	15.128	0.915	0.835	**−0.007**	**0.873**
14	0.208	0.268	0.168	0.652	0.206	18.150	0.877	0.825	0.182	24.670
15	0.156	0.226	0.124	0.611	0.173	15.311	0.913	0.937	0.072	8.966
16	0.156	0.227	0.124	0.612	0.172	15.330	0.913	0.903	0.072	8.918
17	0.157	0.228	0.125	0.617	0.174	15.417	0.912	1.008	0.069	8.432
18	0.170	0.226	0.148	0.605	0.188	15.275	0.913	0.675	0.082	10.299
19	0.172	0.229	0.145	0.608	0.184	15.499	0.911	0.678	0.094	11.993
20	0.176	0.237	0.142	0.603	0.183	16.025	0.904	0.795	0.133	18.047
21	0.176	0.236	0.142	0.602	0.183	15.994	0.905	0.770	0.133	18.012
22	2.490	3.250	1.518	7.572	1.812	220.630	−16.947	9.729	2.490	29.490
23	0.236	0.304	0.165	0.717	0.189	20.612	0.843	0.538	0.225	27.279
24	0.311	0.395	0.196	0.927	0.225	26.804	0.735	0.586	0.297	28.271
25	0.311	0.395	0.196	0.927	0.225	26.804	0.735	0.586	0.297	28.271
26	0.157	0.219	0.105	0.586	**0.131**	14.877	0.918	**0.423**	−0.083	10.085
27	3.005	3.495	1.902	7.692	1.972	237.256	−19.754	4.848	−3.005	41.620
28	0.283	0.371	0.175	0.893	0.211	25.197	0.766	0.526	−0.261	24.475
29	0.176	0.239	0.124	0.608	0.151	16.224	0.903	0.500	0.135	16.879
30	0.217	0.297	0.141	0.754	0.176	20.171	0.850	0.508	−0.169	17.085
31	0.410	0.519	0.259	1.205	0.295	35.252	0.542	0.666	−0.402	30.225
32	0.141	**0.195**	0.118	**0.528**	0.149	**13.273**	**0.935**	0.483	0.063	8.454
33	0.243	0.320	0.208	0.881	0.265	21.698	0.826	0.755	−0.051	3.990
34	0.181	0.239	0.138	0.586	0.164	16.194	0.903	0.512	0.156	21.433
35	0.179	0.236	0.138	0.581	0.164	16.041	0.905	0.511	0.154	21.218
36	0.181	0.238	0.142	0.586	0.170	16.131	0.904	0.509	0.154	21.031
37	0.166	0.225	0.143	0.590	0.180	15.272	0.914	0.594	0.103	12.700
38	0.178	0.240	0.145	0.620	0.177	16.322	0.902	0.697	0.125	15.078
39	0.367	0.440	0.344	0.989	0.442	29.852	0.671	1.325	0.364	36.355
40	0.498	0.570	0.371	1.251	0.389	38.687	0.448	0.646	0.492	42.409
41	0.152	0.222	0.115	0.596	0.155	15.044	0.917	0.555	0.077	9.187
42	0.145	0.210	0.110	0.580	0.147	14.273	0.925	0.504	0.032	3.755
43	0.275	0.361	0.171	0.873	0.205	24.537	0.778	0.523	−0.251	23.828
44	0.145	0.208	**0.104**	0.561	0.136	14.099	0.927	0.488	0.066	8.338
45	0.244	0.307	0.186	0.720	0.218	20.872	0.839	0.574	0.233	28.581
46	0.374	0.547	0.255	1.349	0.351	37.149	0.491	1.795	0.354	20.933
47	0.314	0.404	0.207	0.980	0.241	27.400	0.723	0.652	−0.275	23.066
48	0.422	0.625	0.268	1.541	0.366	42.434	0.336	2.256	0.405	20.991
49	**0.139**	0.200	0.106	0.542	0.142	13.546	0.932	0.500	0.056	7.173
50	0.152	0.219	0.119	0.598	0.160	14.843	0.919	0.546	0.052	6.026

5. *RMSRE*: root mean squared relative error [48,49]

$$\mathrm{RMSRE} = \sqrt{\frac{1}{n}\sum_{i=1}^{n}\left(\frac{\overline{H}_d^{i,m} - \overline{H}_d^{i,c}}{\overline{H}_d^{i,m}}\right)^2} \tag{59}$$

6. *RRMSE*: relative root mean square error. This indicator is calculated by dividing RMSE with average value of measured data. According to [50], model accuracy is considered excellent when RRMSE $< 10\%$, good if $10\% <$ RRMSE $< 20\%$, fair if $20\% <$ RRMSE $< 30\%$, and poor if RRMSE $> 30\%$.

$$\mathrm{RRMSE} = \frac{\sqrt{\frac{1}{n}\sum_{i=1}^{n}\left(\overline{H}_d^{i,m} - \overline{H}_d^{i,c}\right)^2}}{\sum_{i=1}^{n}\overline{H}_d^{i,m}} \times 100 \tag{60}$$

7. *MBE*: mean bias error [37]. This indicator expresses a tendency of model to underestimate (negative value) or overestimate (positive value) horizontal diffuse solar radiation, while the MBE values closest to zero are desirable. The drawback of this test is that it does not show the correct performance when the model presents overestimated and underestimated values at the same time, since overestimation and underestimation values cancel each other:

$$\mathrm{MBE} = \frac{1}{n}\sum_{i=1}^{n}\left(\overline{H}_d^{i,m} - \overline{H}_d^{i,c}\right) \tag{61}$$

8. R^2: coefficient of determination [51]. This indicator is often used in statistics for estimating the performance of the models. It depicts the fraction of the calculated values that are closest to the line of measurement data. While the ideal values of all other statistical indicators used in this study is 0, values of the coefficient of determination close to 1 indicate more efficient models:

$$\mathrm{R}^2 = 1 - \frac{\sum_{i=1}^{n}\left(\overline{H}_d^{i,m} - \overline{H}_d^{i,c}\right)^2}{\sum_{i=1}^{n}\left(\overline{H}_d^{i,m} - \overline{H}_d^{m,avg}\right)^2} \tag{62}$$

Table 7
Statistical indicators for empirical models for climate zone E.

#	MAE	RMSE	MARE	U_{95}	RMSRE	RRMSE	R^2	erMAX	MBE	*t*-stat
1	0.631	0.934	0.253	2.301	0.326	45.628	0.414	0.591	0.622	4.285
2	0.636	0.906	0.254	2.196	0.313	44.247	0.449	0.557	0.636	4.723
3	0.749	1.007	0.318	2.390	0.358	49.208	0.319	0.596	0.749	5.342
4	0.814	1.085	0.336	2.568	0.384	53.030	0.209	0.622	0.814	5.438
5	0.531	0.811	0.215	2.025	0.279	39.623	0.558	0.526	0.515	3.938
6	0.460	0.718	0.187	1.812	0.245	35.068	0.654	0.473	0.435	3.658
7	0.577	0.770	0.241	1.821	0.264	37.601	0.602	0.431	0.577	5.436
8	0.603	0.825	0.252	1.972	0.286	40.322	0.543	0.489	0.603	5.135
9	0.595	0.802	0.248	1.906	0.276	39.185	0.568	0.460	0.595	5.301
10	0.543	0.733	0.224	1.743	0.248	35.823	0.639	0.399	0.543	5.284
11	0.548	0.742	0.279	2.013	0.304	36.260	0.630	0.511	0.260	1.796
12	0.497	0.766	0.200	1.917	0.262	37.406	0.606	0.499	0.481	3.866
13	0.534	0.777	0.216	1.899	0.266	37.979	0.594	0.493	0.532	4.509
14	0.722	0.980	0.300	2.336	0.344	47.898	0.355	0.579	0.722	5.222
15	0.625	0.932	0.253	2.305	0.326	45.552	0.416	0.594	0.614	4.198
16	0.625	0.934	0.255	2.312	0.327	45.619	0.415	0.593	0.612	4.156
17	0.626	0.933	0.261	2.315	0.329	45.597	0.415	0.592	0.607	4.106
18	0.614	0.835	0.258	1.989	0.290	40.770	0.532	0.492	0.614	5.208
19	0.620	0.842	0.256	2.006	0.290	41.140	0.524	0.487	0.620	5.225
20	0.669	0.938	0.268	2.262	0.325	45.841	0.409	0.566	0.669	4.873
21	0.668	0.937	0.267	2.259	0.324	45.764	0.411	0.564	0.668	4.872
22	2.467	2.575	1.034	5.269	1.058	99.078	−3.809	1.512	2.467	11.063
23	0.764	0.833	0.303	1.769	0.307	32.067	0.496	0.375	0.764	7.637
24	0.823	0.878	0.337	1.831	0.343	33.771	0.441	0.424	0.823	8.920
25	0.823	0.878	0.337	1.831	0.343	33.771	0.441	0.424	0.823	8.920
26	0.381	0.438	0.151	0.964	0.161	16.837	0.861	0.230	0.381	5.880
27	3.421	3.713	1.337	7.854	1.348	142.855	−8.998	1.607	−3.421	7.861
28	**0.143**	**0.195**	**0.060**	**0.502**	0.080	**7.489**	**0.973**	0.139	0.112	2.323
29	0.618	0.677	0.247	1.442	0.252	26.044	0.668	0.322	0.618	7.410
30	0.175	0.227	0.077	0.550	0.098	8.727	0.963	0.167	0.162	3.403
31	0.170	0.215	0.068	0.563	**0.078**	8.285	0.966	**0.116**	−0.115	2.090
32	0.682	0.769	0.260	1.674	0.264	29.591	0.571	0.324	0.682	6.358
33	0.267	0.308	0.122	0.865	0.140	11.848	0.931	0.211	**0.057**	**0.622**
34	0.727	0.805	0.283	1.728	0.287	30.973	0.530	0.350	0.727	7.000
35	0.728	0.807	0.283	1.734	0.286	31.039	0.528	0.349	0.728	6.940
36	0.723	0.803	0.280	1.728	0.284	30.892	0.532	0.345	0.723	6.873
37	0.794	0.899	0.299	1.962	0.303	34.587	0.414	0.370	0.794	6.240
38	0.808	0.905	0.308	1.960	0.312	34.818	0.406	0.369	0.808	6.570
39	1.334	1.567	0.477	3.500	0.487	60.276	−0.780	0.617	1.334	5.389
40	1.365	1.523	0.516	3.290	0.518	58.591	−0.682	0.575	1.365	6.698
41	0.948	1.076	0.371	2.352	0.382	41.401	0.160	0.492	0.948	6.184
42	0.903	1.031	0.353	2.263	0.365	39.669	0.229	0.473	0.903	6.019
43	0.210	0.291	0.086	0.703	0.109	11.179	0.939	0.170	0.210	3.460
44	0.674	0.754	0.268	1.630	0.276	28.994	0.588	0.344	0.674	6.629
45	1.208	1.357	0.465	2.945	0.471	52.203	−0.335	0.578	1.208	6.481
46	1.986	2.256	0.791	4.934	0.823	86.800	−2.691	1.143	1.986	6.156
47	0.413	0.544	0.168	1.290	0.197	20.948	0.785	0.296	0.413	3.868
48	0.985	1.076	0.400	2.289	0.410	41.408	0.160	0.512	0.985	7.515
49	0.864	0.979	0.336	2.140	0.345	37.684	0.304	0.440	0.864	6.209
50	1.068	1.223	0.413	2.688	0.425	47.048	−0.084	0.556	1.068	5.958

9. *erMAX*: maximum absolute relative error [52]

$$\mathrm{erMAX} = \max\left(\left|\frac{\overline{H}_d^{i,m} - \overline{H}_d^{i,c}}{\overline{H}_d^{i,m}}\right|\right) \tag{63}$$

10. *t-stat*: *t*-Statistic. This indicator, which had a long history of popular usage, was first proposed by Stone [53] to be used in conjunction with RMSE and MBE for more complete evaluation of solar radiation estimation models. Later on *t*-statistics became a widely accepted test for validating whether or not the calculated values of solar radiation are not significantly different from their measured counterparts [47,46,27,54,55]:

$$t-\mathrm{stat} = \sqrt{\frac{(n-1)\mathrm{MBE}^2}{\mathrm{RMSE}^2 - \mathrm{MBE}^2}} \tag{64}$$

6. Results and discussion

Calculated statistical indicators for different empirical models for climate zones A–E are shown in Tables 3–7. Bold values refer to the most accurate model regarding particular indicator. As it has been said the lower the value the more accurate the estimate. The only exception is indicator R^2, which is higher in more accurate models. The perfect linear relationship between the estimated and measured values is given with R^2 around 1, while values of R^2 around 0 indicate that there is no linear relationship between the estimated and measured values. Due to computational definition of coefficient of determination it is also possible that indicator R^2 be negative, which means that a model fits worse than a horizontal line. Such models are for example 22, 27, 46 and 48 for climate zone C.

Based on selected statistical indicators the most accurate model for climate zone A is model 49, for climate zone B model 30, for

climate zone C model 49, 42 and 44, for climate zone D model 32 and for climate zone E model 30 and 28. However, it is very difficult to qualitative compare or rank large number of models using statistical indicators in tabular form. The more distinct approach is to use visualization technique, by means of which one can get a clear picture of how close a particular model is to measured data and how it is relatively compared to other models. The most widely used visualization technique for comparing predicted and measured values is the scatter plot. However, the scatter plot is not convenient for combining results of more than two models on the same graph. The more convenient visual tool is the Taylor diagram [56], which provides "a concise statistical summary of how well patterns match each other in terms of their correlation, their root-mean-square difference and the ratio of their variances". This diagram has been widely adopted by the climate and geophysics researchers for performing intercomparison studies and producing insightful visualizations [57]. On the other side use of Taylor diagrams in solar radiation studies is very rare [46]. Taylor diagram graphically summarizes how closely model predictions match observations. This is a very useful tool that combines information about the correlation coefficient (R), root mean squared error (RMSE), and standard deviation into a single point on a two-dimensional polar plot that assigns the azimuthal position to the inverse cosine of the correlation coefficient and radial distance from the origin to the standard deviation. The point representing the reference field is plotted along the horizontal axis and the distance of each model on the plot from the reference point quantifies how closely that model matches measurements. Taylor diagrams for analyzed models for five main climate zones are given in Figs. 4–8. The particular advantage of presenting statistical results using Taylor diagrams is that the models are apparently clustered according to their performance. From Taylor diagrams for models applied on locations in climate zone A (Fig. 4) it is seen that bulk of the models are grouped along the same centered RMS line. Models 11 and 45 that have the same RMS error and pretty much the same correlation with observations (0.806 and 0.812 respectively), but model 11 has similar standard deviation as the observed, whereas model 45 has much lower spatial variability (with a standard deviation of 0.288 kWh/m^2 compared to the observed value of 0.485 kWh/m^2). Models 10, 7, 9, 39, 40 and 46 have the worst performance for climate zone A and therefore are located the farthest from the reference point. Models 22, 27 and 38 due to very bad performance fall outside the limits of the graph. For climate zone B (Fig. 5), the models that fall outside the limits of the graph are models 10, 22, 27, and 48. The nearest to the reference point are models 29, 30, 44, 49 and 42 and slightly farther are models 23, 34, 35, 26, 41, 47, 15, 17, 1 and 16. For climate zone C (Fig. 6) the worst models that fall outside the limits of the graph are models 22 and 27. Model 22 with negative correlation ($R=-0.217$) and standard deviation of 3.12 kWh/m^2 is located in the second quadrant, while the model 27 with standard deviation of 2.59 kWh/m^2 and correlation that equals 0.89 is in the first quadrant by far away from the reference point. The nearest to the reference point are models 49, 42 and 44, the representative points of which are very close that almost overlap, which indicates that these models have very similar performance. Slightly weaker performance show models 50, 41, 29, 16, 1, 15 and 17 that are also very close i.e. have very similar performance. For climate zone D

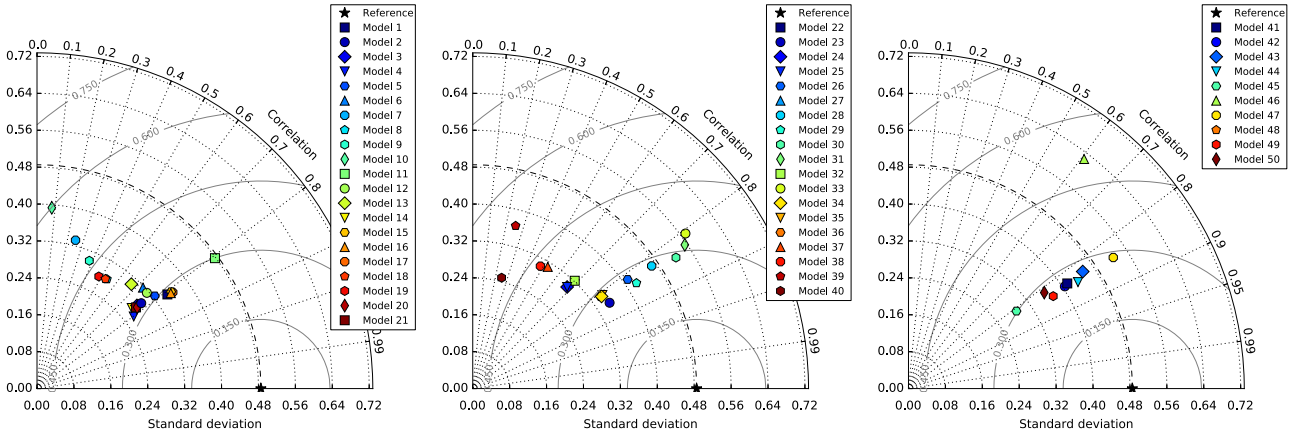

Fig. 4. Taylor diagram for models applied on locations in climate zone A.

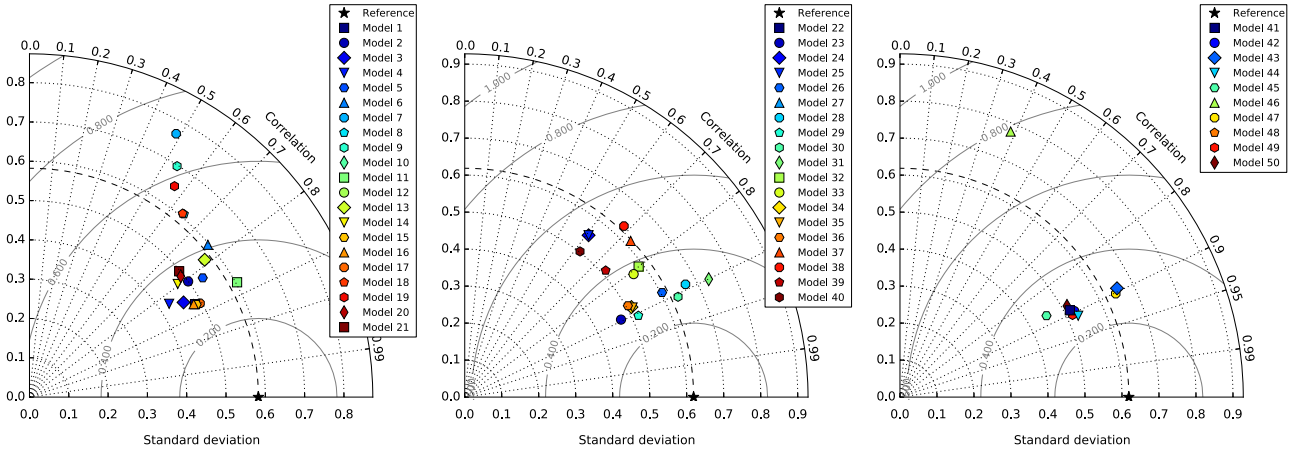

Fig. 5. Taylor diagram for models applied on locations in climate zone B.

(Fig. 7) model 22 with negative correlation ($R=-0.405$) and standard deviation of 1.66 kWh/m^2 is located in the second quadrant, while the model 27 with standard deviation of 2.52 kWh/m^2 and correlation that equals 0.96 is in the first quadrant by far away from the reference point. For this climate zone representative points of many models lie close to each other, but slightly better characteristics show models 2, 32, 34, 35, 36, 49, 44 and 41. For climate zone E (Fig. 8) model 27 falls outside the limits of the graph (standard deviation = 2.71 kWh/m^2, $R=99$). The best performance show models 28 and 30 that almost overlap, and slightly weaker are models 43 and 31.

7. Concluding remarks

This paper gives a statistical evaluation of empirical models for predicting monthly mean horizontal diffuse solar radiation. A total of fifty empirical models found in the literature are used in statistical analysis. The analysis was carried out for five main climate zones according to Köppen–Geiger climate classification. The

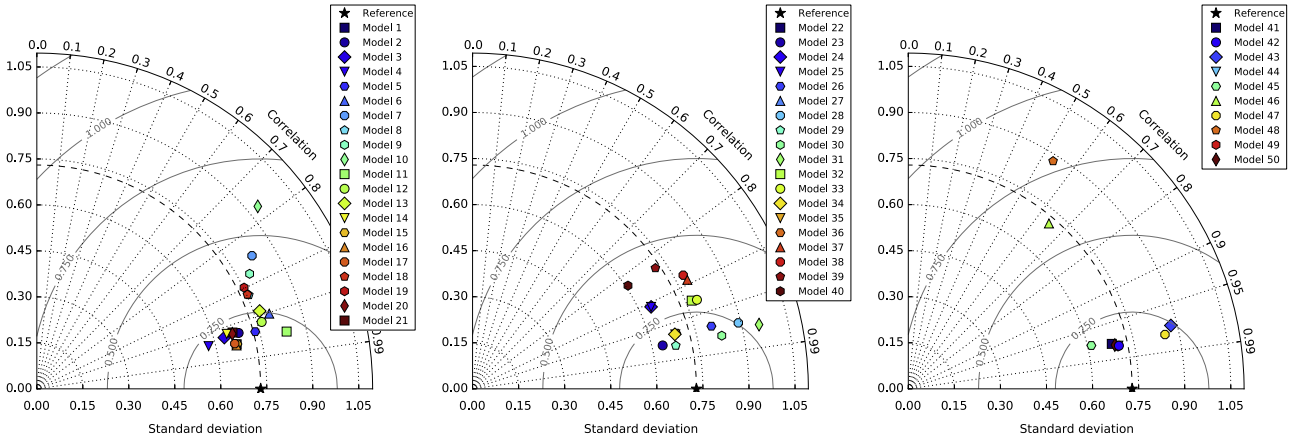

Fig. 6. Taylor diagram for models applied on locations in climate zone C.

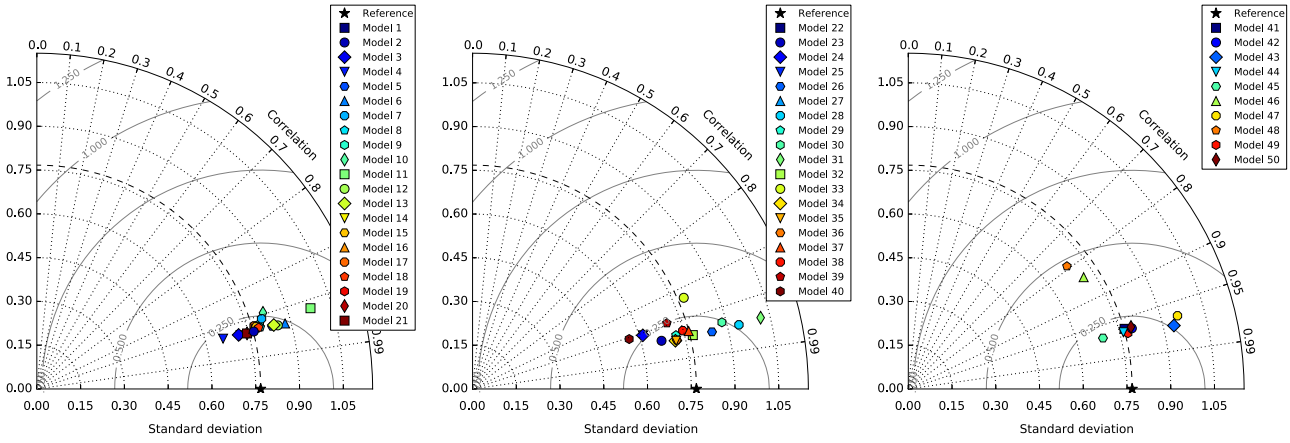

Fig. 7. Taylor diagram for models applied on locations in climate zone D.

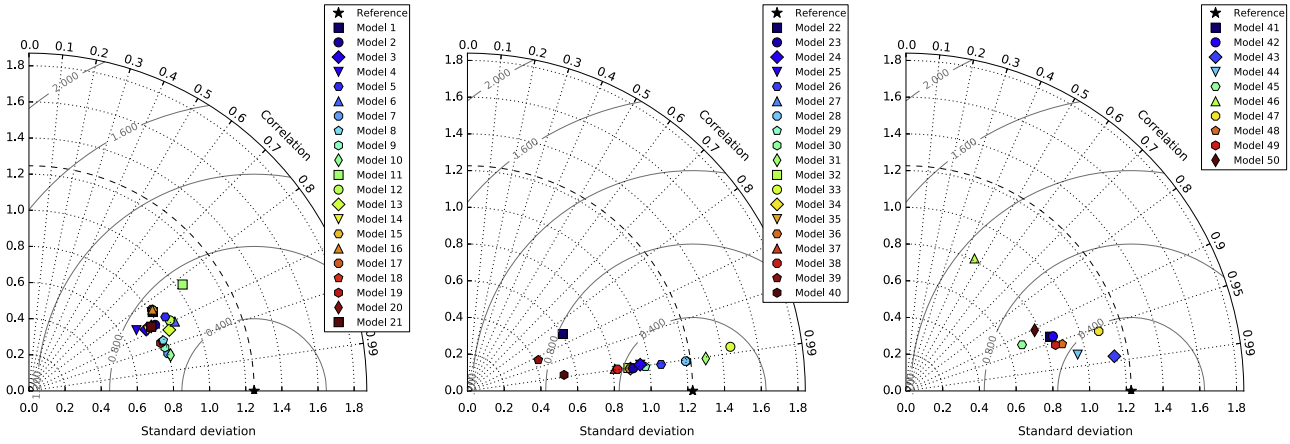

Fig. 8. Taylor diagram for models applied on locations in climate zone E.

models are evaluated using long term meteorological data for 267 different sites. The models are also divided in three groups according to dependent variable(s). The first group consists of 21 models in which the monthly mean diffuse fraction is the function of the monthly mean clearness index. The second group consists of 19 models in which the monthly mean diffuse fraction is the function of the monthly mean relative sunshine duration. The third group consists of 10 models in which the monthly mean diffuse fraction is the function of both, the monthly mean clearness index and the monthly mean relative sunshine duration. Ten statistical quantitative indicators are used to evaluate different diffuse solar radiation models. The results are also visually presented by means of Taylor diagrams, which give a clear picture of how close a particular model is to measured data and how it is relatively compared to other models. In addition, presenting model's performance using Taylor diagram makes it possible to easily cluster models regarding their performance. This makes easier selection of most appropriate model for every climate zone. In addition from Figs. 4–8 it could be concluded that models from second and third group of models offer, in general, better performance comparing the models from the first group, for all climate zones. On the other side, these models are often limited by the lack of availability of clearness index or sunshine duration records.

Acknowledgment

This paper is a result of two investigations: (1) project TR33015 of Technological Development of Republic of Serbia, and (2) project III 42006 of Integral and Interdisciplinary investigations of Republic of Serbia. The authors would like to thank the Ministry of Education and Science of Republic of Serbia for financial support during these investigations.

In addition, authors would like to thank three anonymous reviewers for their constructive suggestions.

References

[1] Besharat F, Dehghan AA, Faghih AR. Empirical models for estimating global solar radiation: a review and case study. Renew Sustain Energy Rev 2013;21:798–821. http://dx.doi.org/10.1016/j.rser.2012.12.043 ⟨http://linkinghub.elsevier.com/retrieve/pii/S1364032112007484⟩.

[2] Bertrand C, Vanderveken G, Journée M. Evaluation of decomposition models of various complexity to estimate the direct solar irradiance over Belgium. Renew Energy 2015;74:618–26. http://dx.doi.org/10.1016/j.renene.2014.08.042 ⟨http://linkinghub.elsevier.com/retrieve/pii/S0960148114005011⟩.

[3] Khalil SA, Shaffie A. A comparative study of total, direct and diffuse solar irradiance by using different models on horizontal and inclined surfaces for Cairo, Egypt. Renew Sustain Energy Rev 2013;27:853–63. http://dx.doi.org/10.1016/j.rser.2013.06.038 ⟨http://linkinghub.elsevier.com/retrieve/pii/S1364032113004152⟩.

[4] Bakirci K. Models for the estimation of diffuse solar radiation for typical cities in Turkey. Energy 2015;82:827–38. http://dx.doi.org/10.1016/j.energy.2015.01.093.

[5] Li H, Bu X, Long Z, Zhao L, Ma W. Calculating the diffuse solar radiation in regions without solar radiation measurements. Energy 2012;44(1):611–5. http://dx.doi.org/10.1016/j.energy.2012.05.033.

[6] Wong L, Chow W. Solar radiation model. Appl Energy 2001;69(3):191–224. http://dx.doi.org/10.1016/S0306-2619(01)00012-5.

[7] Liu BY, Jordan RC. The interrelationship and characteristic distribution of direct, diffuse and total solar radiation. Sol Energy 1960;4(3):1–19. http://dx.doi.org/10.1016/0038-092X(60)90062-1.

[8] Tapakis R, Michaelides S, Charalambides A. Computations of diffuse fraction of global irradiance: part 1 – analytical modeling. Sol Energy 2014, http://dx.doi.org/10.1016/j.solener.2014.10.005, ⟨http://www.sciencedirect.com/science/article/pii/S0038092X14004915⟩.

[9] Li H, Ma W, Wang X, Lian Y. Estimating monthly average daily diffuse solar radiation with multiple predictors: a case study. Renew Energy 2011;36(7):1944–8. http://dx.doi.org/10.1016/j.renene.2011.01.006.

[10] Dervishi S, Mahdavi A. Computing diffuse fraction of global horizontal solar radiation: a model comparison. Sol Energy 2012;86(6):1796–802. http://dx.doi.org/10.1016/j.solener.2012.03.008.

[11] Singh G, Bhatti S. Statistical comparison of global and diffuse solar radiation correlations. Energy Convers Manag 1990;30(2):155–61. http://dx.doi.org/10.1016/0196-8904(90)90027-V.

[12] Magarreiro C, Brito M, Soares P, Azevedo E. Assessment of diffuse radiation models in Azores. Sol Energy 2014;16:5748. http://dx.doi.org/10.1016/j.solener.2014.08.003.

[13] Khorasanizadeh H, Mohammadi K, Mostafaeipour A. Establishing a diffuse solar radiation model for determining the optimum tilt angle of solar surfaces in Tabass, Iran. Energy Convers Manag 2014;78:805–14. http://dx.doi.org/10.1016/j.enconman.2013.11.048.

[14] Torres JL, De Blas M, García A, de Francisco A. Comparative study of various models in estimating hourly diffuse solar irradiance. Renew Energy 2010;35(6):1325–32. http://dx.doi.org/10.1016/j.renene.2009.11.025.

[15] Lee K, Yoo H, Levermore GJ. Quality control and estimation hourly solar irradiation on inclined surfaces in South Korea. Renew Energy 2013;57:190–9. http://dx.doi.org/10.1016/j.renene.2013.01.028.

[16] Duffie J, Beckman W. Solar engineering of thermal processes. New York: A Wiley-Interscience Publication, Wiley; 1991.

[17] Cooper P. The absorption of radiation in solar stills. Sol Energy 1969;12(3):333–46. http://dx.doi.org/10.1016/0038-092X(69)90047-4 ⟨http://www.sciencedirect.com/science/article/pii/0038092X69900474⟩.

[18] Klein S. Calculation of monthly average insolation on tilted surfaces. Sol Energy 1977;19(4):325–9. http://dx.doi.org/10.1016/0038-092X(77)90001-9.

[19] Page JK. The estimation of monthly mean values of daily total short-wave radiation on vertical and inclined surfaces from sunshine records for latitudes 40N–40S. In: Proceedings of UN conference on new sources of energy; 1961. pp. 378–90.

[20] Ibrahim SM. Diffuse solar radiation in Cairo, Egypt. Energy Convers Manag 1985;25(1):69–72. http://dx.doi.org/10.1016/0196-8904(85)90072-X.

[21] Iqbal M. A study of Canadian diffuse and total solar radiation data – I Monthly average daily horizontal radiation. Sol Energy 1979;22(1):81–6.

[22] Tiris M, Tiris C, Türe IE. Correlations of monthly-average daily global, diffuse and beam radiations with hours of bright sunshine in Gebze, Turkey. Energy Convers Manag 1996;37(9):1417–21. http://dx.doi.org/10.1016/0196-8904(95)00227-8.

[23] Bortolini M, Gamberi M, Graziani A, Manzini R, Mora C. Multi-location model for the estimation of the horizontal daily diffuse fraction of solar radiation in Europe. Energy Convers Manag 2013;67:208–16. http://dx.doi.org/10.1016/j.enconman.2012.11.008.

[24] Trabea AA. A multiple linear correlation for diffuse radiation from global solar radiation and sunshine data over Egypt. Renew Energy 1999;17(3):411–20.

[25] Taşdemiroğlu E, Sever R. Estimation of monthly average, daily, horizontal diffuse radiation in Turkey. Energy 1991;16(4):787–90. http://dx.doi.org/10.1016/0360-5442(91)90030-P.

[26] Aras H, Balli O, Hepbasli A. Estimating the horizontal diffuse solar radiation over the Central Anatolia Region of Turkey. Energy Convers Manag 2006;47(15–16):2240–9. http://dx.doi.org/10.1016/j.enconman.2005.11.024.

[27] Ulgen K, Hepbasli A. Diffuse solar radiation estimation models for Turkey's big cities. Energy Convers Manag 2009;50(1):149–56. http://dx.doi.org/10.1016/j.enconman.2008.08.013.

[28] Tarhan S, Sari A. Model selection for global and diffuse radiation over the Central Black Sea (CBS) region of Turkey. Energy Convers Manag 2005;46(4):605–13. http://dx.doi.org/10.1016/j.enconman.2004.04.004.

[29] Barbaro S, Cannata G, Coppolino S, Leone C, Sinagra E. Diffuse solar radiation statistics for Italy. Sol Energy 1981;26(5):429–35. http://dx.doi.org/10.1016/0038-092X(81)90222-X.

[30] Pandey CK, Katiyar AK. A comparative study to estimate daily diffuse solar radiation over India. Energy 2009;34(11):1792–6. http://dx.doi.org/10.1016/j.energy.2009.07.026.

[31] Lewis G. Diffuse irradiation over Zimbabwe. Sol Energy 1983;31(1):125–8.

[32] Gopinathan KK. Computing the monthly mean daily diffuse radiation from clearness index and percent possible sunshine. Sol Energy 1988;41(4):379–85.

[33] Rensheng C, Ersi K, Jianping Y, Shihua L, Wenzhi Z, Yongjian D. Estimation of horizontal diffuse solar radiation with measured daily data in China. Renew Energy 2004;29(5):717–26. http://dx.doi.org/10.1016/j.renene.2003.09.012.

[34] Said R, Mansor M, Abuain T. Estimation of global and diffuse radiation at Tripoli. Renew Energy 1998;14(1-4):221–7. http://dx.doi.org/10.1016/S0960-1481(98)00071-8.

[35] Sabzpooshani M, Mohammadi K. Establishing new empirical models for predicting monthly mean horizontal diffuse solar radiation in city of Isfahan, Iran. Energy 2014;69:571–7. http://dx.doi.org/10.1016/j.energy.2014.03.051.

[36] Boukelia TE, Mecibah MS, Meriche IE. General models for estimation of the monthly mean daily diffuse solar radiation (Case study: Algeria). Energy Convers Manag 2014;81:211–9. http://dx.doi.org/10.1016/j.enconman.2014.02.035.

[37] Jiang Y. Estimation of monthly mean daily diffuse radiation in China. Appl Energy 2009;86(9):1458–64. http://dx.doi.org/10.1016/j.apenergy.2009.01.002.

[38] Gopinathan K, Soler A. Diffuse radiation models and monthly-average, daily, diffuse data for a wide latitude range. Energy 1995;20(7):657–67 ⟨http://EconPapers.repec.org/RePEc:eee:energy:v:20:y:1995:i:7:p:657-667⟩.

[39] Elminir HK, Azzam YA, Younes FI. Prediction of hourly and daily diffuse fraction using neural network, as compared to linear regression models. Energy 2007;32(8):1513–23. http://dx.doi.org/10.1016/j.energy.2006.10.010.

[40] Li H, Ma W, Lian Y, Wang X, Zhao L. Global solar radiation estimation with sunshine duration in Tibet, China. Renew Energy 2011;36(11):3141–5. http://dx.doi.org/10.1016/j.renene.2011.03.019.

[41] Mustafa Omer A. Diffuse solar radiation over Shambat, Khartoum North. Renew Energy 1994;4(2):227–33. http://dx.doi.org/10.1016/0960-1481(94)90008-6.
[42] Kottek M, Grieser J, Beck C, Rudolf B, Rubel F. World map of the Köppen-Geiger climate classification updated. Meteorol Z 2006;15(3):259–63. http://dx.doi.org/10.1127/0941-2948/2006/0130.
[43] WRDC, World Radiation Data Centre, World Meteorological Organization, ⟨http://wrdc-mgo.nrel.gov/⟩; 2015.
[44] Willmott CJ, Matsuura K. Advantages of the mean absolute error (MAE) over the root mean square error (RMSE) in assessing average model performance. Clim Res 2005;30(1):79–82 http://dx.doi.org/10.3354/cr030079.
[45] Yadav AK, Chandel S. Solar radiation prediction using artificial neural network techniques: a review. Renew Sustain Energy Rev 2014;33:772–81. http://dx.doi.org/10.1016/j.rser.2013.08.055 ⟨http://linkinghub.elsevier.com/retrieve/pii/S1364032113005959⟩.
[46] Gueymard CA. A review of validation methodologies and statistical performance indicators for modeled solar radiation data: towards a better bankability of solar projects. Renew Sustain Energy Rev 2014;39:1024–34. http://dx.doi.org/10.1016/j.rser.2014.07.117 ⟨http://linkinghub.elsevier.com/retrieve/pii/S1364032114005693⟩.
[47] Behar O, Khellaf A, Mohammedi K. Comparison of solar radiation models and their validation under Algerian climate - The case of direct irradiance. Energy Convers Manag 2015;98:236–51. http://dx.doi.org/10.1016/j.enconman.2015.03.067 ⟨http://linkinghub.elsevier.com/retrieve/pii/S019689041500285X⟩.
[48] Göçken M, Özçalici M, Boru A, Dosdogru AT. Integrating metaheuristics and artificial neural networks for improved stock price prediction. Expert Syst Appl 2015, http://dx.doi.org/10.1016/j.eswa.2015.09.029, ⟨http://linkinghub.elsevier.com/retrieve/pii/S0957417415006570⟩.
[49] Webber H, Martre P, Asseng S, Kimball B, White J, Ottman M, et al., Canopy temperature for simulation of heat stress in irrigated wheat in a semi-arid environment: a multi-model comparison, Field Crop Res, http://dx.doi.org/10.1016/j.fcr.2015.10.009, ⟨http://dx.doi.org/10.1016/j.fcr.2015.10.009⟩.
[50] Li MF, Tang XP, Wu W, Liu HB. General models for estimating daily global solar radiation for different solar radiation zones in mainland China. Energy Convers Manag 2013;70:139–48. http://dx.doi.org/10.1016/j.enconman.2013.03.004.
[51] Yorukoglu M, Celik AN. A critical review on the estimation of daily global solar radiation from sunshine duration. Energy Convers Manag 2006;47(15-16):2441–50. http://dx.doi.org/10.1016/j.enconman.2005.11.002.
[52] Elagib NA, Mansell MG. New approaches for estimating global solar radiation across Sudan. Energy Convers Manag 2000;41(5):419–34. http://dx.doi.org/10.1016/S0196-8904(99)00123-5.
[53] Stone R. Improved statistical procedure for the evaluation of solar radiation estimation models. Sol Energy 1993;51(4):289–91. http://dx.doi.org/10.1016/0038-092X(93)90124-7.
[54] Al-Mostafa Z, Maghrabi A, Al-Shehri S. Sunshine-based global radiation models: a review and case study. Energy Convers Manag 2014;84:209–16. http://dx.doi.org/10.1016/j.enconman.2014.04.021.
[55] Yao W, Li Z, Wang Y, Jiang F, Hu L. Evaluation of global solar radiation models for Shanghai, China. Energy Convers Manag 2014;84:597–612. http://dx.doi.org/10.1016/j.enconman.2014.04.017.
[56] Taylor KE. Summarizing multiple aspects of model performance in a single diagram. J Geophys Res 2001;106(D7):7183–92. http://dx.doi.org/10.1029/2000JD900719.
[57] Correa C, Lindstrom P. The mutual information diagram for uncertainty visualization. Int J Uncertain Quantif 2012;3(3):187–201. http://dx.doi.org/10.1615/Int.J.UncertaintyQuantification.2012003959.